Proposed Model to Study Behaviors Stand-Alone Induction Generator Driven by Wind Energy System Under Different Loading and Excitation Fluctuation

Hayder Hussein Kadhum
College of *Engineering/University of Babylon/, Babylon, Iraq*
eng.hayder.kadhum@uobabylon.edu.iq

Abstract

this paper attention is focused on the performance of dynamic modeling of stand-alone self-excited induction generator (SEIG) when driven with wind energy system using state-space approach . The proposed dynamic model consists of induction generator; self excitation capacitance and load model are expressed in stationary d-q reference frame with the actual saturation curve of the machine. The performance of SEIG is investigated under (no load, balanced and unbalanced R-L/R-C loads) with different excitation fluctuation. The new proposed modal can also examines the dynamic performances of the generator during sudden and reduction of load. and variation of excitation capacitance value by considering the effect of main and cross-flux saturation. In previous literature there is no discussion about the performance of SEIG system under all various conditions as mentioned above. The performance of SEIG system is simulated using MATLAB/SIMULINK and the simulation results demonstrates the feasibility of the proposed model. This method may be used for low cost variable speed wind energy conversion systems.

Key words: Stand-Alone, Induction Generator, Wind Energy System

نموذج مقترح لدراسة سلوك مولد حثي يقاد بنظام طاقة الرياح في ظل تقلبات التحميل و تحت تقلب الإثارة المختلفة

حيدر حسين كاظم
جامعة بابل/كلية الهندسة/ العراق/ حله

الخلاصة

هذا البحث يُركِّزُ الاهتمام على أداءَ العرض الديناميكي لمولّدِ الحثِّ الذاتي المستقلِ عندما يقادَ بنظامِ طاقةِ الرياح. النموذج المُقتَرَح يَشْملُ مولّدِ الحثِّ، متسعة إثارة ونموذج حمل ممثل ب(d-q) ومنحنى الإشباعِ الفعلي للمولّد. إنّ الأداءَ لديناميكي للمولّدِ تم بحثه تحت الشروط (لا حملَ، حمل مقاومه ومحاثة ومقاومه ومتسعة متوازنة وكذألك حمل مقاومه ومحاثة ومقاومه ومتسعة غير متوازنة) تحت تقلب الإثارة المختلفة . النموذج المقترح بإمكانه أيضا اختبار أداء المولد أثناء القطع المفاجئِ منْ الحمــلِ الــساكنِ والديناميكي وتغير في قيمة متسعة الأثارة أخذا بعين الاعتبار تأثيرِ الإشباعِ الرئيسي . في البحوث السابقة ليس هناك مُناقشة حول أداءِ نظامِ مولّدِ الحثِّ الذاتي المــستقلِ تحــت كــل الــشروطِ المُخْتَلفــةِ كمــا هــو مــذكور أعــلاه. تــم اســتخدام برنــامج (MATLAB/SIMULINK) في أداء المولد ونَتائِج المحاكاةَ تبرهن ملائمة عمل النموذجِ المُقتَرَحِ. هذه الطريقةِ قَدْ تُستَعملُ لتقليل كلفة تحويل سرعةِ الرياح المتغيّرة .

الكلمات المفتاحية: مولد حثي، قائم بذاته، نظام طاقة الرياح

I. Introduction

Energy demand of the world is increasing year by year. With the increasing demand of energy, besides of the exploitation of the traditional sources, new energy sources are searched and used throughout the world depending upon their availability and their relative benefits. Within the new energy sources wind energy can play a significant role in solving the world energy problem **N. H. Malik and S. E. Haque**

1986. It is a clean and abundant resource that can produce electricity with no pollutant gas emission. Induction generators are widely used for wind powered electric generation, especially in remote areas, because they do not need an external power supply to produce the excitation magnetic field. An induction generator offers various advantages over the conventional synchronous generators such as reduced unit cost, easy maintenance, rugged and simple construction, brushless rotor (squirrel cage) and so on **D. Seyoum, C. Grantham and F. Rahman 2002**. It is well known that a three-phase induction machine can be made to work as a self-excited induction generator (SEIG) **S.S. Mutthy, B. Singh, S. Gupta and B.M. Gulat, 2003**. In an isolated application an induction generator operates in the self-excited mode by connecting the capacitors to the stator terminals. In a grid connected induction generator the magnetic field is produced by excitation current drawn from the grid. In recent years, self-excited induction generator has been widely used as such as in hydroelectric and wind energy applications, **Ahmet Caliskan**,**2005**.Robust and brushless construction (squirrel cage rotor), low maintenance requirements, absence of DC power supply for field excitation, small seize, reduced cost, better transient performance, self-protection against short-circuits and large over loads, are some of the advantages of the induction generator over the synchronous and DC generators. Because this advantages widely used in stand-alone wind power generation schemes **Kyoungsoo Ro Han-ho Choi**,**2005 and Ali Nesba[1], Rachid Ibtiouen[2] 2006**.Two models are reported in literature for the analysis of self-excited induction machine. One is based on the per-phase equivalent approach and the other, the d-q axis model, is based on the generalized machine theory. Most of the work is based on per-phase equivalent circuit approach, which includes loop-impedance method and the nodal admittance method **Harish Kumar, Neel Kamal, 2011and** Mohamed Mansour, M. **N. Mansouri , M.F. Mmimouni**,**2011.** The d-q method has been used by Elder et al. and others. Self excited phenomenon in induction generator has been well documented **Youcef Bekakra, Djilani Ben attous,2011.**Proposed a generalized state-space dynamic modeling of a three phase SEIG has been developed using d-q variables in stationary reference frame for transient analysis. The modeling of excitation system under balanced/un-balanced conditions has been developed in terms of d-q. Different constraints such as variation of excitation, wind speed and load have been taken into account and accordingly the effect on generated voltage and current has been analyzed **M.Sasikumar and S.Chenthur Pandian,2010**. The effect of excitation capacitance on generated voltage has been analyzed. The aim of this paper is to present an analysis of the dynamic performance of an isolated three-phase SEIG feeding four types of three-phase static loads; resistive (R), resistive-inductive (RL), resistive-capacitive (RC) and resistive inductive-capacitive loads. The dynamic flux models of the SEIG as well as the models of R, RL, RC and loads are given **Tilak Thakur and Shailendra Kumar Gupta**,**2012**. The analysis presented is validated by experimental results.

2.Seig Modeling

The d-q axes equivalent circuit of a (SEIG) supplying an Resistive load is shown in Fig.1 classical matrix formulation using d-q axes modeling is used to represent the dynamics of conventional induction machine operating as a generator. Using such a matrix representation, one can obtain the instantaneous voltages and currents during the self excitation process, as well as during load variations.

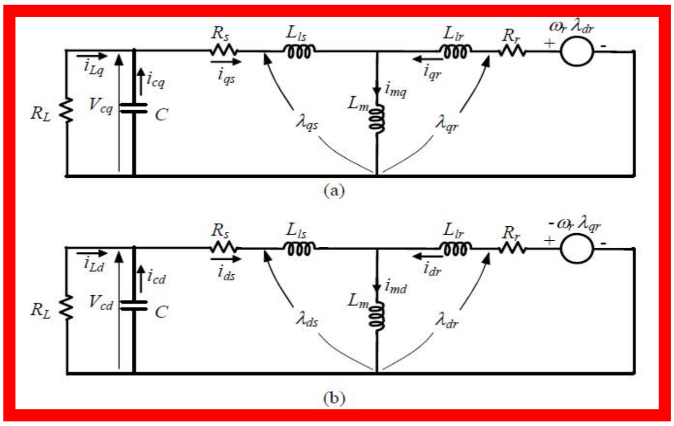

Fig. 1. d-q model of a loaded SEIG in a stationary reference frame (a) q-axis circuit (b) d-axis circuit

2.1 Self-Excitation capacitor and load model

2.1.1 Capacitor model:

The equations (1) and (2) represents the self excitation capacitor currents and voltages in d-q axes representation

$$V_{cd} = \frac{1}{C}\int i_{cd}\,dt + V_{cd}\,|_{t=0} \qquad \text{-(1)}$$

$$V_{cq} = \frac{1}{C}\int i_{cq}\,dt + V_{cq}\,|_{t=0} \qquad \text{-(2)}$$

Where:

$V_{cd} = V_{ds}$, $V_{cq} = V_{qs}$

$i_{cd} = i_{ds} - i_{Ld}$

$i_{cq} = i_{qs} - i_{Lq}$

Where Vcd |t=0, Vcq |t=0, are the initial voltages of the self-excitation capacitor without which voltages cannot be build up in SEIG. The SIMULINK model of excitation capacitor is shown in Fig.2.This model describes the capacitor model for both balanced and unbalanced excitation conditions.

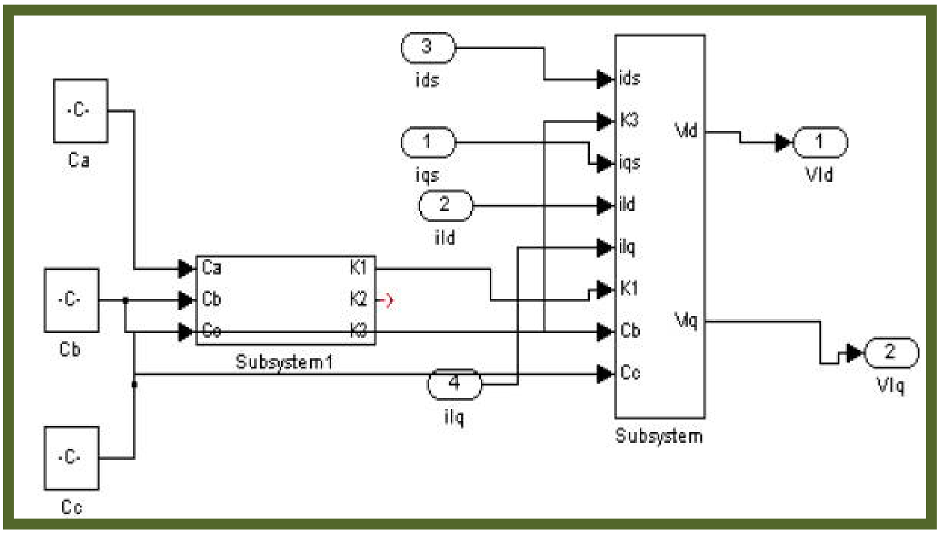

Fig. 2 Simulink Model of excitation Capacitor (balanced/ un-balanced self-excitation)

This is the total block diagram of capacitor model. has been implemented by using equations from (1) and (2) this consists of two subsystems. The developed model in SIMULINK for excitation is the proposed new model based on the derived equations. The variation of the magnetizing inductance, measured at rated frequency, for the induction machine used in this investigation is given in Fig. 3, where the dots are experimental results and the curve is a fourth order curve fit given by

$$L_m = -1.62\times10^{-11}V_{ph}^4 + 2.67\times10^{-8}V_{ph}^3 - 1.381\times10^{-5}V_{ph}^2 + 1.76\times10^{-3}V_{ph} + 0.23 \quad \text{-(3)}$$

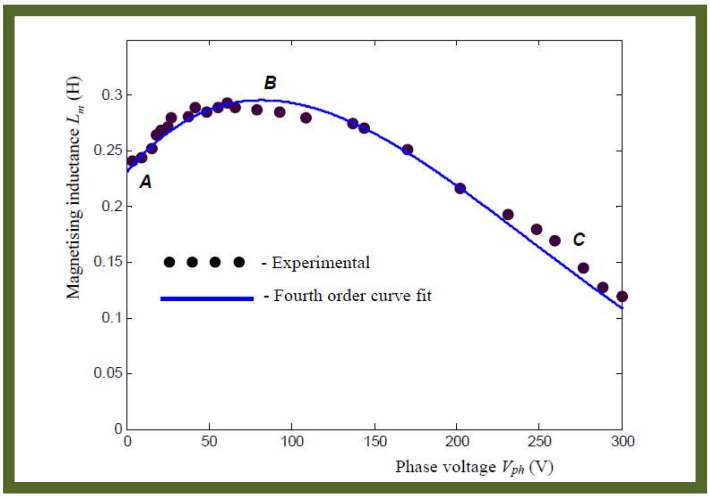

Fig. 3 Variation of magnetizing inductance with phase voltage at rated frequency

2.1.2- SEIG Operation With Static Load

$$\frac{d}{dt}i_{ld} = \frac{1}{L}v_{ld} - \frac{R}{L}i_{ld} \;,\; \frac{d}{dt}i_{lq} = \frac{1}{L}v_{lq} - \frac{R}{L}i_{lq} \quad (4)$$

$$v_{ld} = Ri_{ld} + L\frac{d}{dt}i_{ld} \;,\; v_{lq} = Ri_{lq} + L\frac{d}{dt}i_{lq} \quad (5)$$

Equations (4) and (5) represents the d-q axes load voltages and currents: Here the modeling of load has been developed in terms of d-q reference frame under balanced /un-balanced conditions as shown in fig (4). The load currents in terms of their respective voltages have been discussed in below

A) Balanced Inductive load:

The dynamic model of a three-phase balanced series RL (resistive-inductive) load in the β-α axis stationary reference frame is expressed by

$$\frac{di_{L\alpha}}{dt} = (v_\alpha - Ri_{L\alpha})/L$$

$$\frac{di_{L\beta}}{dt} = (v_\beta - Ri_{L\beta})/L .$$

And can be excreted by d-q reference frame

$$i_{1d} = V_{1d}/Ra,\ I_{1q} = V_{1q}/R \qquad -(6)$$

B) Unbalanced Inductive load

$$i_{1d}=\int((1/La)V_{1d} -(Ra/La)i_{1d}),$$
$$i_{1q}=(2/\sqrt{3})[(-R_a/L_a) +(R_b/L_b)]i_{1d} -(R_b/L_b)i_{1q} - (2/\sqrt{3}L_b)V_{1d} + (2/\sqrt{3}L_a)V_{1d} + (1/L_b)\, V_{1q} \qquad -(7)$$

C) Balanced Resistive load

The model of a three-phase balanced resistive load in the β-α axis stationary reference frame is given by:

And can be excreted by d-q reference frame

$$i_{1d}=\int((1/L)V_{1d} -(R/L)i_{1d}),\ i_{1q}=\int((1/L)V_{1q}-(R/L)i_{1q} \qquad -(8)$$

$$v_\alpha = Ri_{L\alpha} ,$$

$$v_\beta = Ri_{L\beta} ,$$

D)Unbalanced Resistive load

can be excreted by d-q reference frame

$$i_{1d} = V_{1d}/Ra \quad i_{1q} = 0.5773502(1/R_a -1/R_b)V_{1d} + V_{1q}/R_b \qquad -(9)$$

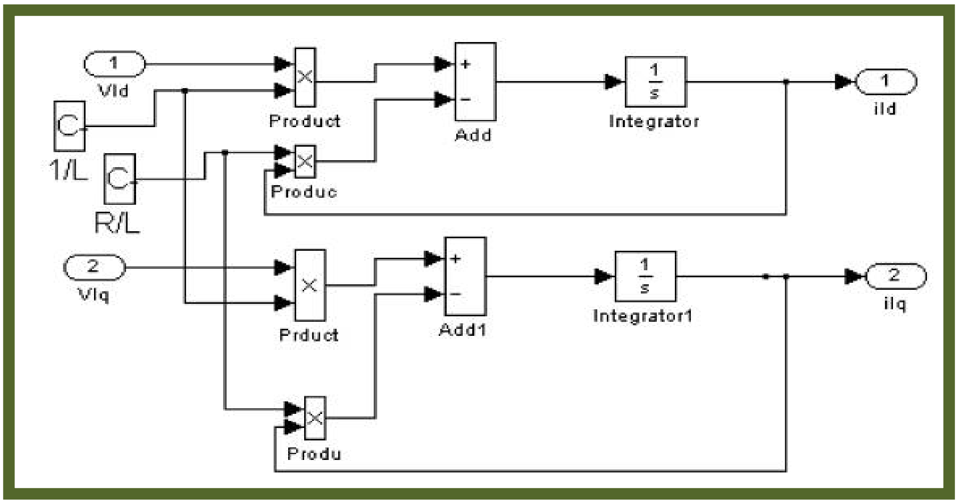

(10)

Fig 4. Block model of Resistive and Inductive –load

2.2 SEIG Operation with dynamic Load:

The dynamic model of three-phase squirrel cage induction motor as dynamic load is similar to that of the induction generator but the parameters concerned is related to the motor. The complete dynamic model is represented by the set of eight differential equations corresponding to variables as shown in equation (11) is the generalized state space representation of a SEIG model. That is in the form of classical state-space equation

$$p[x]=[A][x]+[B][u],\ \text{or:}$$
$$p\begin{bmatrix} i_G \\ v_C \\ i_L \end{bmatrix}=\begin{bmatrix} G \\ C \\ L \end{bmatrix}\begin{bmatrix} i_G \\ v_C \\ i_L \end{bmatrix}+[B][v_G] \tag{11}$$

$$\begin{bmatrix} v_{ds} \\ v_{qs} \\ v_{dr} \\ v_{qr} \end{bmatrix}=\begin{bmatrix} R_s+L_s p+\left(\dfrac{R+Lp}{RCp+LCp^2+1}\right) & 0 & L_m p & 0 \\ 0 & R_s+L_s p+\left(\dfrac{R+Lp}{RCp+LCp^2+1}\right) & 0 & L_m p \\ L_m p & \omega_r L_m & R_r+L_r p & \omega_r L_r \\ -\omega_r L_m & L_m p & -\omega_r L_r & R_r+L_r p \end{bmatrix}\begin{bmatrix} i_{ds} \\ i_{qs} \\ i_{dr} \\ i_{qr} \end{bmatrix} \tag{12}$$

$$p\begin{bmatrix} i_{ds} \\ i_{qs} \\ i_{dr} \\ i_{qr} \\ \hdashline v_{Ld} \\ v_{Lq} \\ \hdashline i_{Ld} \\ i_{Lq} \end{bmatrix} = K\left\{ \left[\begin{array}{cccc:cc:cc} R_sL_r & -\omega L_m^2 & -R_rL_m & -\omega L_mL_r & L_r & 0 & 0 & 0 \\ \omega L_m^2 & R_sL_r & \omega L_mL_r & -R_rL_m & 0 & L_r & 0 & 0 \\ -R_sL_m & \omega L_mL_s & R_rL_s & \omega L_sL_r & -L_m & 0 & 0 & 0 \\ -\omega L_mL_s & -R_sL_m & -\omega L_sL_r & R_rL_s & 0 & -L_m & 0 & 0 \\ \hdashline 1/CK & 0 & 0 & 0 & 0 & 0 & -1/CK & 0 \\ 0 & 1/CK & 0 & 0 & 0 & 0 & 0 & -1/CK \\ \hdashline 0 & 0 & 0 & 0 & 1/LK & 0 & -R/LK & 0 \\ 0 & 0 & 0 & 0 & 0 & 1/LK & 0 & -R/LK \end{array}\right] \begin{bmatrix} i_{ds} \\ i_{qs} \\ i_{dr} \\ i_{qr} \\ \hdashline v_{Ld} \\ v_{Lq} \\ \hdashline i_{Ld} \\ i_{Lq} \end{bmatrix} + \left[\begin{array}{cccc} -L_r & 0 & L_m & 0 \\ 0 & -L_r & 0 & L_m \\ L_m & 0 & -L_s & 0 \\ 0 & L_m & 0 & -L_s \\ \hdashline 0 & 0 & 0 & 0 \\ 0 & 0 & 0 & 0 \\ \hdashline 0 & 0 & 0 & 0 \\ 0 & 0 & 0 & 0 \end{array}\right] \begin{bmatrix} v_{ds} \\ v_{qs} \\ v_{dr} \\ v_{qr} \end{bmatrix} \right\} \tag{12}$$

The simultaneous solution of this system of equation can be obtained using the Runge-kutta 4th order integration method with automatic adjustment of step. This gives the instantaneous values of d-q axes voltages and currents for stator and rotor. The following assumptions are made in this analysis:

1-Core and mechanical losses in the machine are neglected.

2 All machine parameters, except the magnetizing inductance (Lm), are assumed to be constant.

3-Stator windings, self-excitation capacitors and the load are star connected.

The variation of the magnetizing inductance is the main factor in the dynamics of the voltage build up and stabilization in SEIG. The relationship between magnetizing inductance (Lm) and magnetizing current (Im) for induction machine was obtained experimentally. The non linear relationship between Lm and Im is given as:

$$L_m = -6.89\times10^{-6} I_m^4 + 1.38\times10^{-4} I_m^3 - 1.22\times10^{-3} I_m^2 + 1.28\times10^{-3} I_m + 4.62\times10^{-2}\,\mathrm{H} \tag{13}$$

Where Im is given as

$$I_m = \sqrt{\left(i_{ds} + i_{dr}\right)^2 + \left(i_{qs} + i_{qr}\right)^2} \tag{14}$$

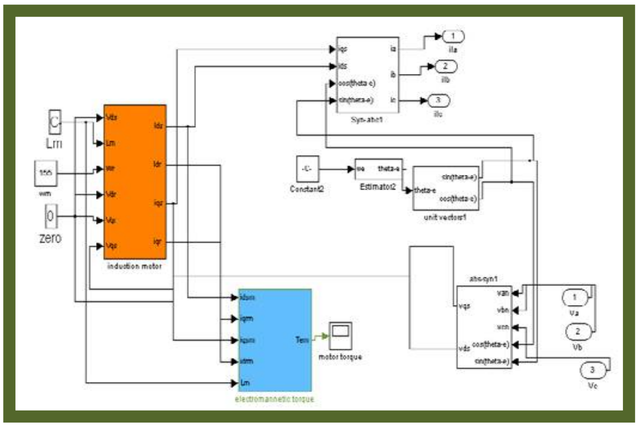

Fig.5 SIMULINK model of dynamic load

2.2 Power characteristics of the wind turbine

Like other substances, the moving air caused from the variations of the air pressure and temperature has the kinetic energy. The relationship of the kinetic energy, *E*, of the flowing air mass ***m***, with velocity $\mathbf{v_W}$ can be expressed as[4]

$$E = \frac{1}{2} m v_w^{\ 2} \tag{15}$$

The instantaneous power of the wind flowing through an area can be expressed as

$$P_{wind} = \frac{dE}{dt} = \frac{1}{2} \rho_{air} \cdot A_v \cdot v_w^3 \tag{16}$$

is the mass density of the flowing air In the light of variable speed wind turbines, the rotor blades rotate freely in accordance with the speed and direction of the wind. The power extracted from the wind is dependent on the rotor power efficiency to capture the wind power. This is based on the fact that the speed of the wind after passing the rotor blades cannot be zero velocity leading to efficiency less than 1. This has nothing to do with the efficiency of the generator. Refer to Betz limit or Betz law, the mechanical power captured by the wind turbine depends on the rotor power efficiency of the turbine $\mathbf{c_p}$ as shown below:

$$P_{tur} = \frac{1}{2} C_p(\lambda) \cdot \rho_{air} \cdot A_v \cdot v_w^3 \tag{17}$$

The rotor power efficiency of the turbine ***Cp*** is the function of the blade tip speed ratio **λ** and blade pitch angle **β**. Equation 18 and 19 express the relationship of **β, λ** ***,and Cp*** with a graph illustrated in figure 9

$$C_p(\lambda,\beta) = 0.5176(\frac{116}{\lambda_i} - 0.4\beta - 5) \cdot e^{-\frac{21}{\lambda_i}} + 0.0068\lambda \tag{18}$$

$$\frac{1}{\lambda_i} = \frac{1}{\lambda + 0.08\beta} - \frac{0.035}{\beta^3 + 1} \tag{19}$$

The maximum rotor power efficiency, regardless of the configurations, is 0.593 [5]. After passing rotor blades, the downstream wind has lower speed and energy. Therefore, wind turbines in a wind farm affect each other. Wind turbines, typically, are located apart from the others three times of their rotor radius to avoid the wake effect [6]. If the tip speed ratio is less than 3, the wake effect reduces the maximum rotor power efficiency further [5]. The tip speed ratio can be calculated from:

$$\lambda = \frac{\omega_b R}{v_w} \tag{20}$$

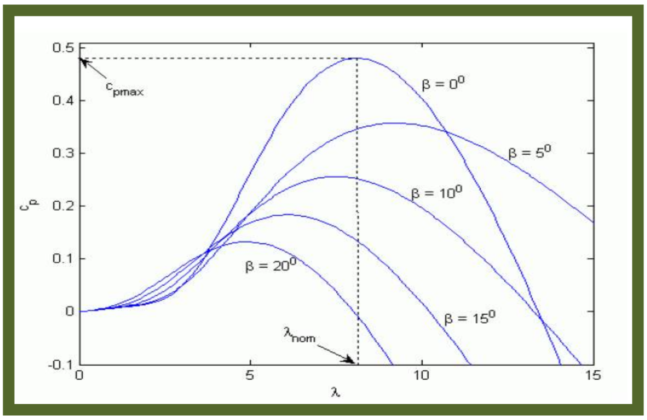

Fig 6. Rotor power efficiency vs. Tip speed ratio

2.4 Torque developed by a wind turbine

The torque in a wind turbine is produced due to the force created as a result of pressure difference on the two sides of each blade of the wind turbine. From fluid mechanics it is known that the pressure in fast moving air is less than in stationary or slow moving air. This principle helps to produce force in an aero plane or in a wind turbine [12]. The mechanical torque can be excreted by [14]

$$t_m = 0.5\rho A(0.5176(\frac{116}{\lambda} - 9.06)e^{\frac{-21}{\lambda}+0.735} + 0.0068\lambda)v_w^{\ 3}\,\frac{R}{G\lambda v_w} \tag{21}$$

The SIMULINK model of wind turbine is shown in Fig.7

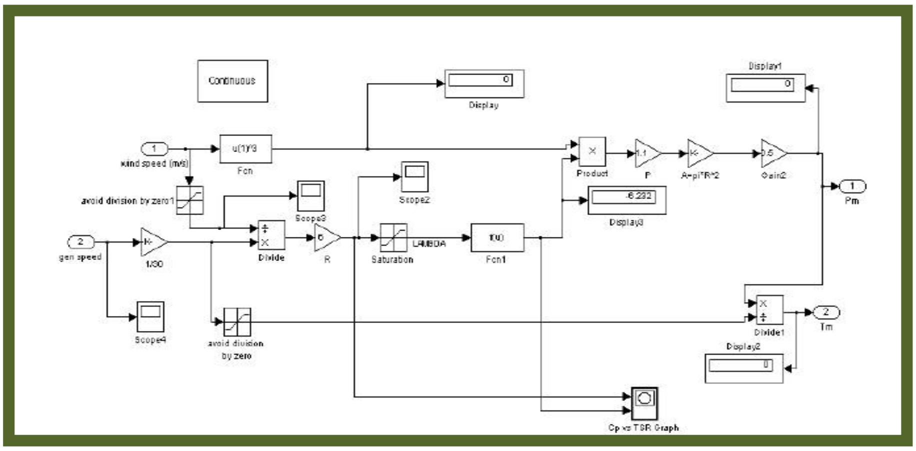

Fig 7. Custom wind turbine model (Air Density: 1.1 kpa)

3. Simulink Model Of Seig

Simulation and the equations described above has been implemented in MATLAB/SIMULINK. The equations from (1) to (12) have been implemented in subsystem. The completed data of the simulation machine is shown in **Table-1.**The excitation and load model is implemented in subsystem 'excitation and Load' as shown in **Fig 8** .Equation (11) shows the eight first order differential equations, for which the solutions gives the four currents (stator d-q axis currents and rotor d -q axis currents), load currents and capacitor voltages. Further these currents are the function of constants viz. stator and rotor inductances, resistances, speed, excitation capacitance and load impedance. And also variables like magnetizing inductance, magnetizing currents and electromagnetic torque generated, has been evaluated using (13) to (21). The constraints of non linear magnetizing inductance has been taken into account, the curve between non linear magnetizing inductance verse phase voltage at rated is shown in Fig 3. The equation (3) of this nonlinear graph has been obtained by curve fitting and hence fourth order nonlinear polynomial equation which is showing the relation between magnetizing inductance verse Magnetizing current.

Table 1. Induction Machine(1) Rating and Parameters

Machine Rating			Number of poles	R_r	R_s	X_r	X_s	X_m	J
HP	Volt	Hz		Ohms	Ohms	Ohms	Ohms	Ohms	$Kg.m^2$
5	415	50	4	1.6	2.75	3.76	3.76	56.83	0.23

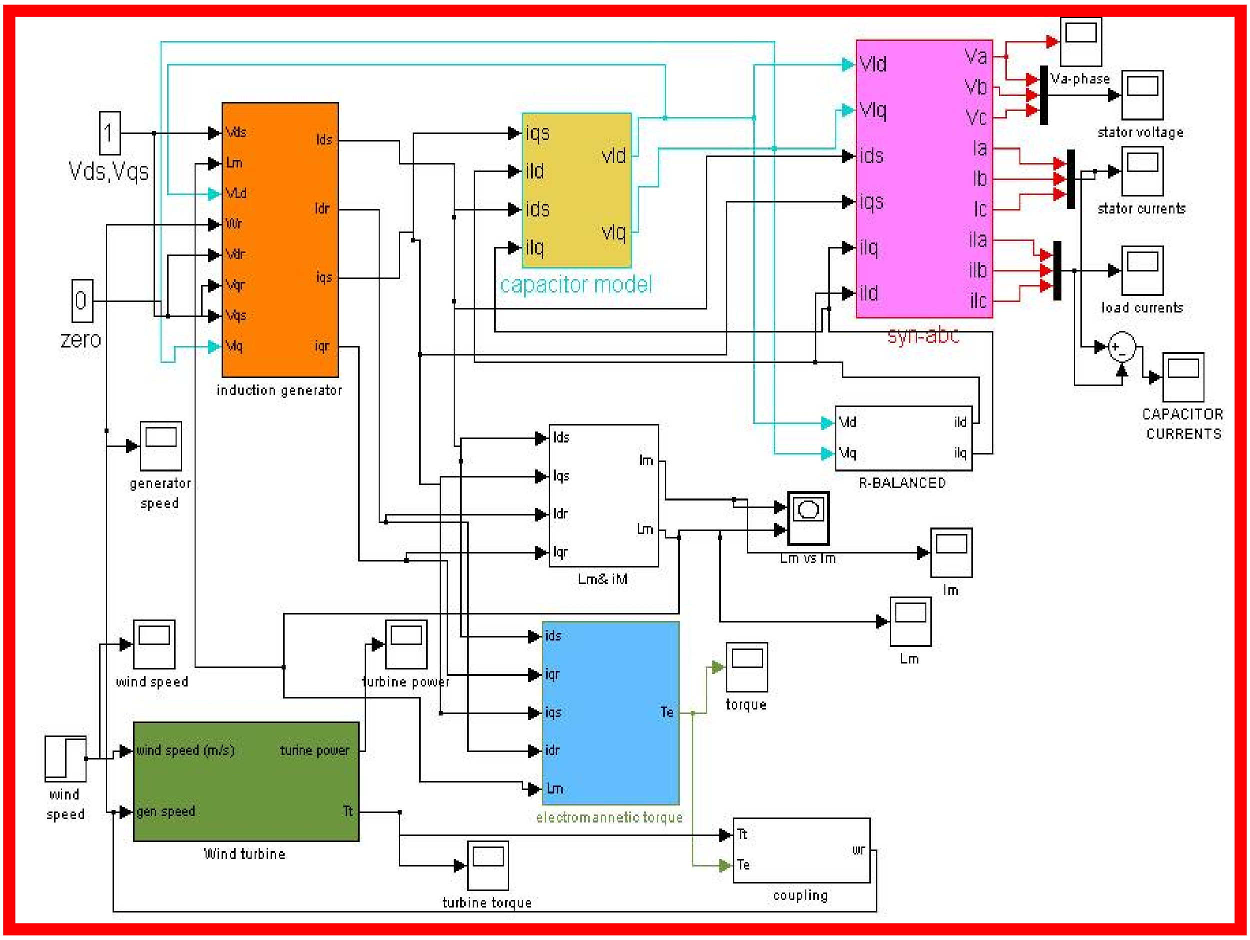

Fig.8 complete proposed model of wind driven SEIG with different load

4. Results And Analysis

Fig. 9 shows the build-up of d-axis stator flux-linkage and q-axis stator flux-linkage during the self-excitation process as a function of time in a three dimensional plot. The flux-linkages continue to grow until they reach their steady state values which are the saturated flux-linkages. The peak values of the d-axis flux-linkage and the q-axis flux linkage are equal. The results of the dynamic self-excitation process given in the previous figures are based on remnant or residual flux in the iron core providing the initial condition required by the self-excited induction generator. When the initial conditions for self excitation are satisfied the flux grows and associated with the growth of flux linkage the generated voltage also grows. The self-excitation process can be also initiated with a charged capacitor. A charged capacitor will provide magnetizing current to the induction generator and the flux and the terminal voltage will grow.

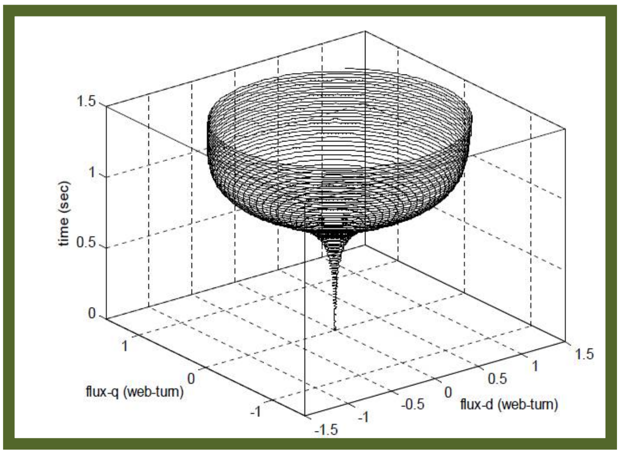

fig. 9 Three dimensional d-axis flux-linkage and q-axis flux-linkage as a function of time during self-excitation process

Fig. 10 shows the transient response of the system on the sudden application and removal of load after the SEIG is brought up to rated voltage at no load. As can be seen, the voltages and currents settle to respective new steady state values, revealing the high over load capability and good transient stability of the SEIG. For this load, the winding current and the load voltage are 5amp and 320volts, respectively. Again, during application and removal of the load, there is no severe voltage/current dip/overshoot. In the Fig. (a) is the generated voltage of the induction generator, (b) is the line current of the induction generator. The application of load is between 0.4 to 0.6secs.

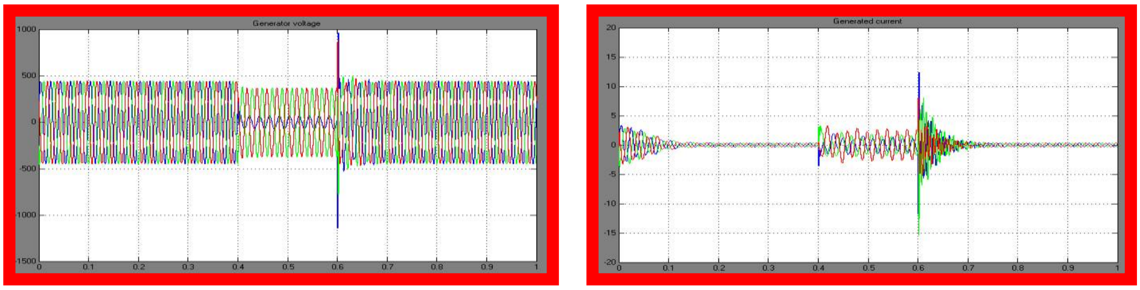

(a)Generated voltage **(b) Line current**

Fig.10.Response of SEIG under load perturbation condition

Figs.11 shows the transient responses of simulated results of the loaded SEIG subject to a sudden Switching off the self excited capacitor under the loading conditions .From these figure we can clear that the responses of case connected to, quickly reach zero value at about t =1.2sec.When the excitation capacitor is switched off, the capacitive load provides some limited source of excitation and thus time delays the transition from saturated state and the corresponding changes in Xm. For this case the self excitation capacitance is disconnected from the machine after it reaches steady state condition. Since the excitation capacitance is disconnected the machine lost its generating mode. Hence the speed is decreased from the super synchronous speed to the speed of the wind turbine. Because of the lost of generating mode now the generated voltage and line current is also becoming zero. Due to this the active and reactive power is also zero. The response curves of the taken condition are as shown in the fig.6.Capacitors are disconnected **at t=0.3sec**. In this figure (a) represent the generated voltage of the induction generator, (b) represent the line current of the induction generator and (c) shows the relation between the load voltage and load current of the induction generator

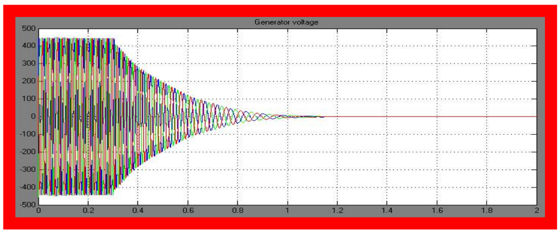

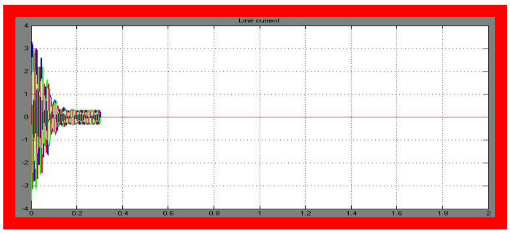

(a)Generated voltage b) Line current

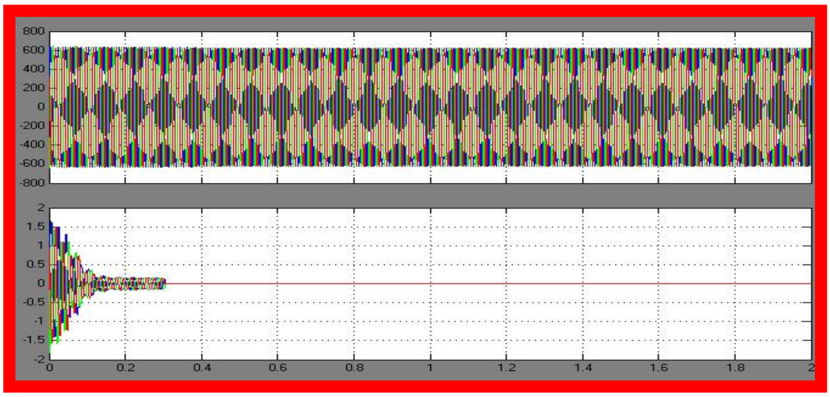

(c)Load voltage and load current

Fig.11.Response of SEIG under sudden disconnection self excitation capacitance

Fig 12. (a) Shows the generated voltage of the induction generator, (b) the line current of the induction generator and (c) the load voltage and load current of the induction generator. The short circuit is applied at t=0.3sec and reaches to zero voltage at t=0.3sec. From these figures we can clearly find out that the responses of case of sudden short circuit at machine terminals, quickly voltage reach to zero value at about t =0.3sec.And after that the machine will not be recovered till the end of the operation.

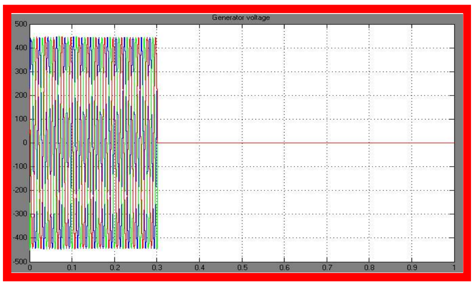

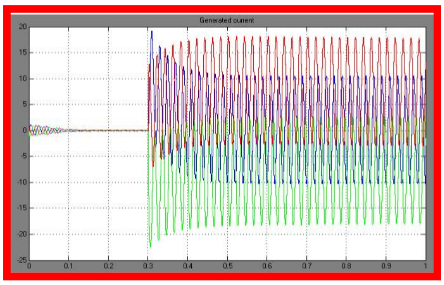

(a) Generated voltage b) Line current

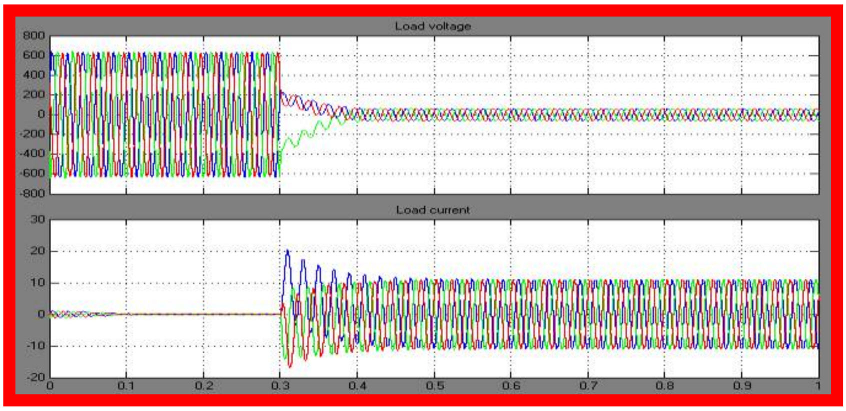

(c) Load voltage and load current

Fig.12.Response of SEIG under sudden disconnection of load

Fig.13 Balanced excitation with No-Load: When generator is excited with capacitance value C=300 μF and rotor speed increased from zero to 2100 rmp in 0.8 sec, the generated voltage and current attains its steady state value of 400 Volts and 21.3 amp in 4.3 sec.

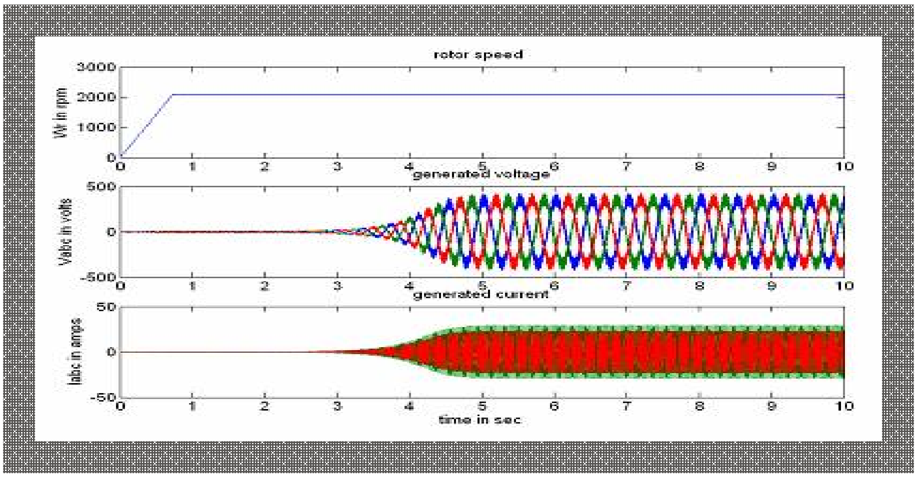

Fig.13. Excitation with no load and C=300 μF

Also in this paper, the results have been determined for SEIG with R-L loads taken under balanced conditions with balanced and unbalanced excitation. The different cases taken for the study are:

Case 1: Balanced Load with balanced excitation: When machine is already heavily loaded (R=39Ω and L=14.5mH) and excited with the capacitance value of C=280 μF and the rotor speed is increased from zero to 2100 rpm. The full self-excitation is taking place in 4.6sec and steady state voltage and current is 400 V and 21.2 Amp respectively as shown in **Fig.14**. With the same capacitance value and with RL load(R=170 Ω and L=46.5mH) and the rotor speed is varied from 1680 rpm to 2100 rpm at t=0 sec. The full self excitation time is reduced from 4.4 sec to 3.2 sec, with the same voltage and currents, as shown in **Fig.15**. With the heavy loaded machine it takes more time to full excitation hence transient time increases.

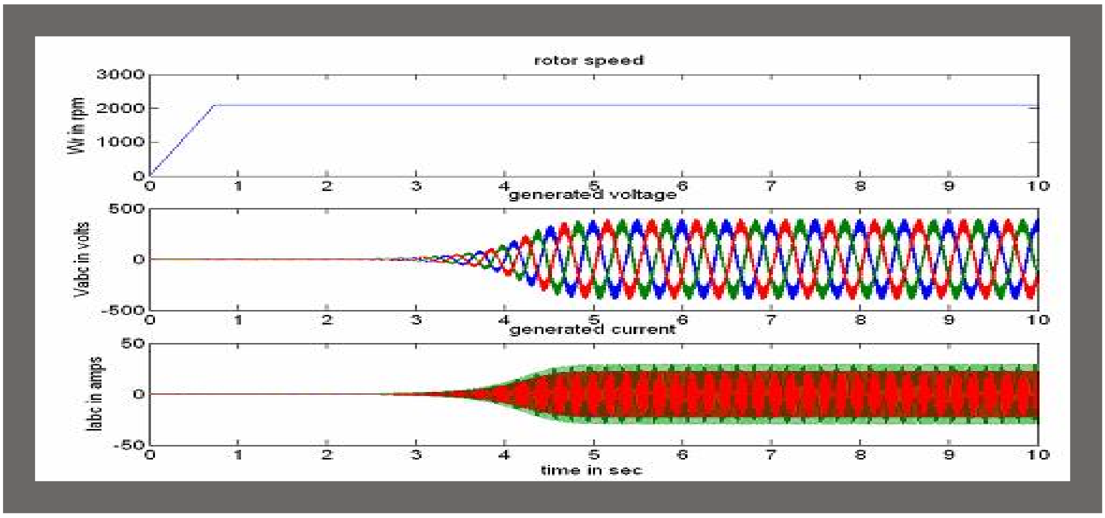

Fig.14. Balanced excitation with balanced RL load(R=39Ω and =14.5mH)

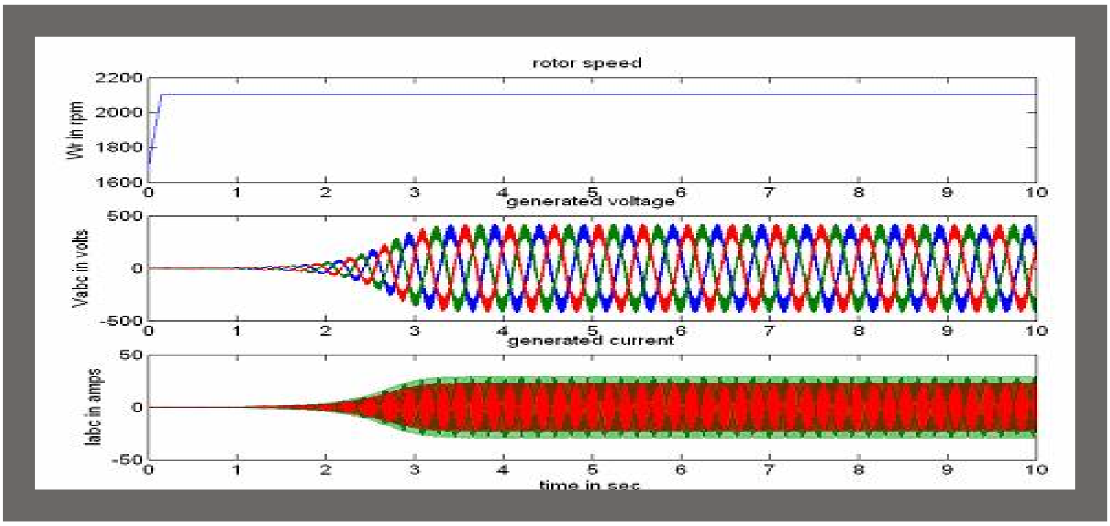

Fig 15. Balanced excitation with balanced RL load (R=170 Ω and L=46.5mH)

Case 2: Variations of Load after Full-Excitation: The machine is first run as a induction motor and it is made to run as a induction generator (rotor speed increased from zero to 2100 rpm i.e. above synchronous speed) with the excitation capacitance of C= 300 μF, the full excitation attains at time t = 4.6 sec. The RL load (R=130 Ω and L=44.5mH) at t = 7 sec is applied. It is observed that the voltage has slightly dropped from 400V to 380V and it is maintaining it as shown in **Fig(.16)**.When the RL load (R=18 Ω and L=10.5mH) applied at t = 7 sec with above mentioned operating conditions, the voltage is decreased from 400V to 310V, as shown in

Fig.(17). When a heavy RL load (R=0.5 Ω and L=1mH) switched on after full excitation at time t = 7 sec, the voltages collapsing completely as shown **in Fig.(18**) By adopting the suitable voltage regulator the voltage can be maintained accordingly.

Fig.16 With RL Load(R=130 Ω and L=44.5mH) at t = 7 sec.

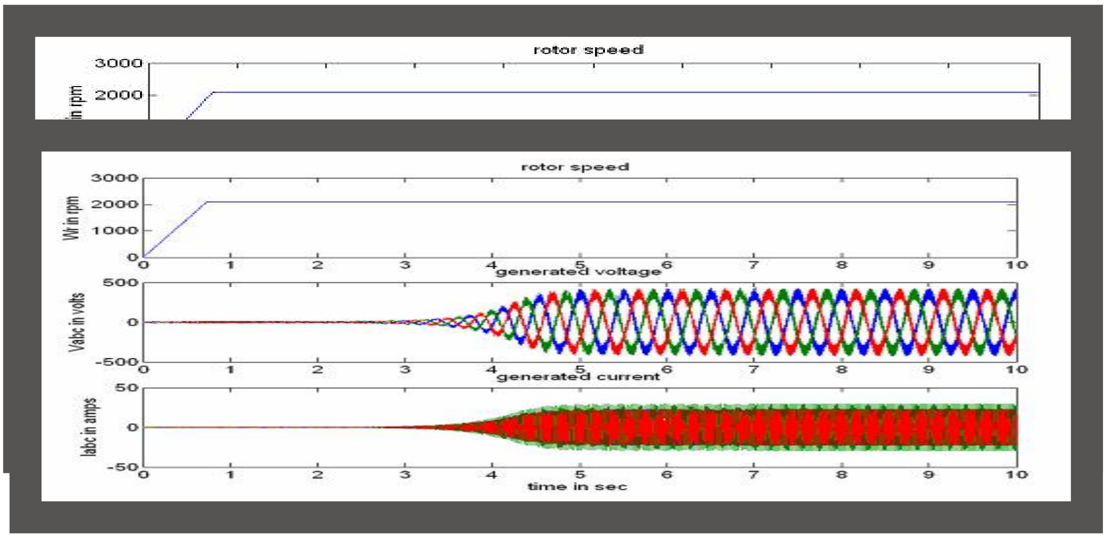

Fig. 17. With RL Load(R=18 Ω and L=10.5mH) at t = 7 sec.

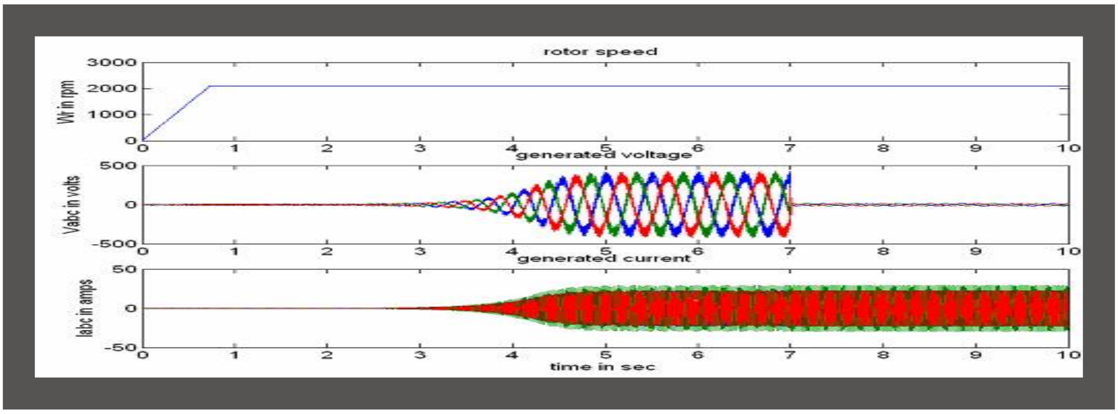

Fig.18. With RL Load(R=0.5 Ω and L=1 mH) at t = 7 sec.

Case 3 : Voltage Collapse and Re-Excitation: When the machine is running at 1760 rpm and its voltage is 400 volts, The RL load(R=100 Ω and L=10mH) is switched on at time t = 3 sec. The voltage is collapsing at time t = 4 sec .i.e. voltage collapsing period is 1 sec. If the machine is excited at time t = 3.6 sec with the capacitance C= 290 µF, and rotor speed is increased to 2100 rpm, the re-excitation (voltage build up) taking place at time t = 9 sec as shown in **Fig. 19**.The excitation period is 5.4 sec. when a light load (R = 260 Ω and L=45.5 mH) is switched on at time

t = 3 sec the complete voltage collapsing period is 0.6 sec (i.e. from 3.0 sec to 3.6 sec). Before the voltage collapses, if the machine is excited at time t = 3.2 sec with capacitance of C = 290 µF and rotor speed is increased to 2100 rpm, the full

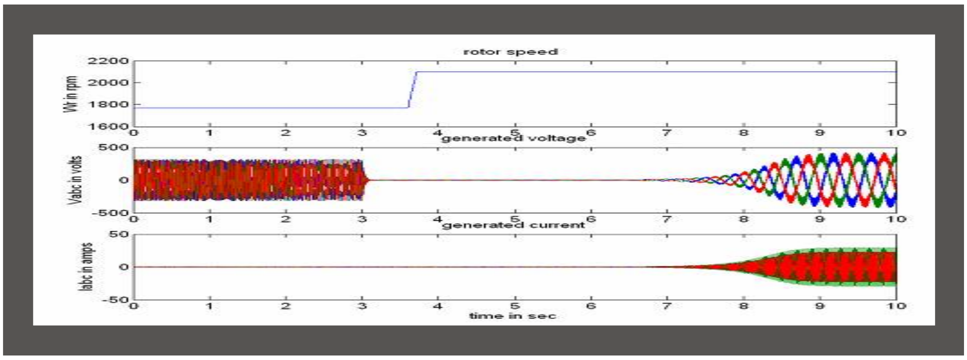

excitation is attained at time t=8.2 sec as shown in **Fig.(20)**. The excitation period is 5 sec. To re-excite the machine, the excitation has to be applied before complete voltage collapse otherwise it will not build up the voltage. As the time gap between switching on load and re-excitation is less(before voltage collapse) the faster the full re excitation of the machine

Fig.19. Voltage collapse and re-excitation with RL load (R=100 Ω and L=10mH).

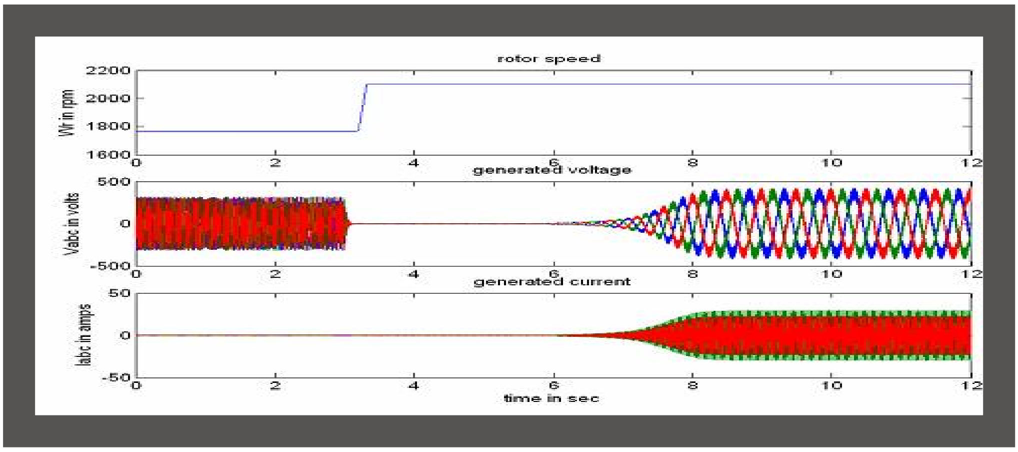

Fig 20. Voltage collapse and re-excitation with RL load (R=260 Ω and L=45.5 mH).

Fig.22. depicts the typical wind turbine torque-speed characteristics for different wind speed. The torque developed by the wind turbine is dependent on the wind speed and the angular rotor speed of the wind turbine. By this characteristic, in this paper the investigation is to see the dynamic effect of the variation in rotor speed on the generated voltage of the SEIG.

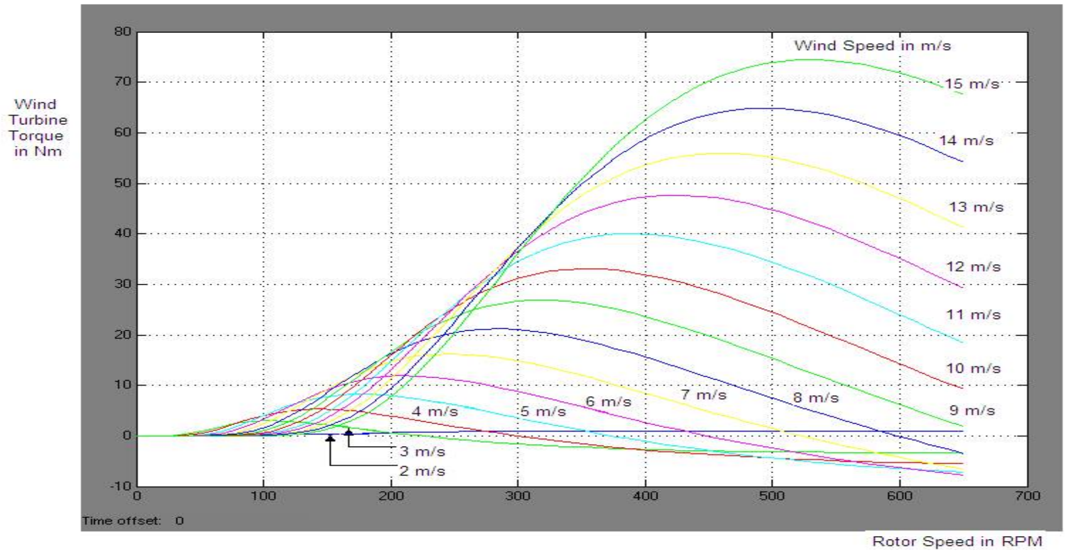

Fig 22 Simulation results of the wind turbine output torque as a function of rotor speed

4. Conclusion

#- In this paper the performance of SEIG has been determined for five different cases. It is observed that the performance of SEIG under balanced R-L and R-C and balanced excitations, the stator voltage, stator currents, load currents and capacitor currents are balanced. In this case the voltage build up is quite fast because of balanced excitation.

#- If the generator operates in the unstable region, the generated voltage will collapse and it loses its eminent magnetic flux. Once the remnant magnetic flux is lost the induction machine has to be run as a motor, or excite the windings from a DC source or the capacitors should be pre-charged to enable the onset of self excitation

#-The connection of a load onto the SEIG terminals causes its excitation to decrease and thus, the SEIG to operate at lower magnetizing flux. The SEIG output voltage is highly influenced by the impedance and the power factor of the load

#- Under un-balanced excitation the electromagnetic torque is having oscillations compared to the case with balanced excitation and capacitor currents are unbalanced.

Under un-balanced load and balanced excitation the electromagnetic torque have more oscillations and are more as compared to other case.

#-With un-balanced exaction and balanced dynamic load, the stator currents and capacitor currents are un-balanced and load currents are balanced. also the voltage is balanced.

The use of series capacitor with the load, improves considerably the output voltage characteristic of the SEIG. This series capacitor must have an adequate capacitance value.

References

N. H. Malik and S. E. Haque, “Steady state analysis and performance of an isolated self-excited induction generator”, IEEE trans. On Energy Conversion, Vol. EC-1, No.3, pp.134-139, September 1986

D. Seyoum, C. Grantham & F. Rahman, “The dynamic analysis and control of a self-excited induction generator driven by a wind turbine”, Proceedings IEEE-IAS, USA, Oct. 2002

S.S. Mutthy, B. Singh, S. Gupta and B.M. Gulati," General steady-state analysis of three-phase self excited induction generator feeding three-phase unbalanced load/single-phase load for stand-alone applications" IEE Pwc.-Gener. Tnmxni Disirik, Vol. 150, No. 1, January ,2003

Ahmet Caliskan, "Constant voltage constant ftequency operation of a self –excited indication generator ", Ph.D. Thesis, September ,2005.

Kyoungsoo Ro Han-ho Choi" Application of neural network controller for maximum power extraction of a grid-connected wind turbine system" Electrical Engineering (2005) 88: 45–53

Ali Nesba1, Rachid Ibtiouen2, Omar Touhami3," Dynamic Performances of Self-Excited Induction Generator Feeding Different Static Loads," Serblan journal of electrical engineering ,Vol. 3, No. 1, June 2006,

Fayez F. M. El-Sousy†, Mohamed Orabi and Hatem Godah, "Maximum Power Point Tracking Control Scheme for Grid Connected Variable Speed Wind Driven Self-Excited Induction Generator", Journal of Power Electronics, Vol. 6, No. 1, January 2006

Thant Zin Soe,"Design and Evaluation of Self Excited Induction Generator for Renewable Energy Systems (Wind Power Generation),", International Conference on Sustainable Development: Issues and Prospects for the GMS 12-14, Nov, 2008.

M.Sasikumar1 and S.Chenthur Pandian2,"Performance Characteristics of Self-Excited Induction Generator fed Current Source Inverter for Wind Energy Conversion Applications" ,International Journal of Computer and Electrical Engineering, Vol.2, No.6, December, 2010 1793-8163

Harish Kumar, Neel Kamal," STEADY STATE ANALYSIS OF SELF-EXCITED INDUCTION GENERATOR," International Journal of Soft Computing and Engineering (IJSCE) ISSN: 2231-2307, Volume-1, Issue-5, November 2011

Mohamed Mansour, M. N. Mansouri , M.F. Mmimouni," Study and Control of a Variable-Speed Wind-Energy System Connected to the Grid ", International Journal Of Renewable Energy Research, IJRER Vol.1, No.2, pp.96-104 ,2011

Youcef Bekakra, Djilani Ben attous,"Active and Reactive Power Control of a DFIG with MPPT for Variable Speed Wind Energy Conversion using Sliding Mode Control", World Academy of Science, Engineering and Technology 60 2011.

S. W. Mohod1, M. V. Aware2,"Laboratory development of wind turbine simulator using variable speed induction motor", International Journal of Engineering, Science and Technology Vol. 3, No. 5, 2011, pp. 73-82.

Tilak Thakur and Shailendra Kumar Gupta," Modeling of a Stand-Alone Induction Generator on Load Using MATLAB Simulink",,Journal of Emerging Trends in Engineering and Applied Sciences (JETEAS) 3 (4): 729-733 ,2012.

BINDESHWAR SINGH1," STAND ALONE POWER GENERATION BY ASYNCHRONOUS GENERATOR: A COMPREHENSIVE SURVEY 3φ"International Journal of Reviews in Computing, 31st July Vol. 10, 2012.